CMLS, Cell. Mol. Life Sci. 1984–1995
1420-682X/05/171984-12
DOI 10.1007/s00018-005-5196-y

CMLS Cellular and Molecular Life Sciences

Research Article

The peptidylarginine deiminases expressed in human epidermis differ in their substrate specificities and subcellular locations

M. C. Méchin[a], M. Enji[b], R. Nachat[a], S. Chavanas[a], M. Charveron[c], A. Ishida-Yamamoto[d], G. Serre[a], H. Takahara[b] and M. Simon[a,*]

[a] CNRS-University of Toulouse III, UMR 5165, Faculté de Médecine, 37 alleés J. Guesde, 31073 Toulouse (France), Fax: +33 5 6114 5938, e-mail: msimon@udear.cnrs.fr
[b] Department of Applied Biological Resource Sciences, School of Agriculture, Ibaraki University, Ami-machi, Inashiki-gun, Ibaraki 300-0393 (Japan)
[c] Institut de Recherche Pierre Fabre, 31052 Toulouse (France)
[d] Department of Dermatology, Asahikawa Medical College, Midorigaoka-Higashi 2-1-1-1, Asahikawa, 078-8510 (Japan)

Received 10 May 2005; received after revision 21 June 2005; accepted 29 June 2005
Online First 9 August 2005

Abstract. Deimination, a post-translational modification catalyzed by peptidylarginine deiminases (PADs), appears as a crucial Ca^{2+}-dependent event in the last steps of epidermal differentiation. In normal human epidermis, where the deiminated proteins are filaggrin and keratins, PAD1, 2 and 3 are expressed but their relative role is unknown. The three PADs, produced as active recombinant forms, showed distinct synthetic-substrate specificities, various efficiencies to deiminate filaggrin and particular calcium and pH sensitivities. Immunoelectron microscopy demonstrated that PAD1 and PAD3 are co-located with filaggrin within the filamentous matrix of the deeper corneocytes where the protein is deiminated. This result strongly suggests that both isoforms are involved in the deimination of filaggrin, an essential step leading to free amino acid production necessary for epidermal barrier function. Moreover, PAD1 was shown to persist up to the upper corneocytes where it deiminates keratin K1, a modification supposed to be related to ultrastructural changes of the matrix.

Key words. Post-translational modification; skin; keratinocyte; differentiation; calcium; citrulline.

The epidermis is a vital tissue since its major function is to protect the organism against physical, chemical and biological aggressions from the environment. The barrier function of the epidermis is linked to a finely regulated equilibrium between proliferation/differentiation of keratinocytes (90 % of the epidermal cells) and desquamation of corneocytes, the terminally differentiated keratinocytes, at the upper surface of the skin [1]. The integrity and homeostasis of the epidermis are known to be dependent on the hydration of the stratum corneum (SC), the outermost cell layer of the epidermis [2]. The hydration is controlled by the natural moisturizing factor (NMF), a complex mixture of small hygroscopic molecules, mainly amino acids and their derivatives. These are directly generated from the catabolism of a single protein abundant in the epidermis, filaggrin.

Filaggrin is a histidine-rich protein synthesized in the cytoplasm of the stratum granulosum (SG), the last living-cell layer under the SC. It is stored in the so-called keratohyalin granules as a high molecular-mass phosphorylated precursor (more than 400 kDa in humans), profilaggrin [3]. After dephosphorylation, the precursor

* Corresponding author.

is proteolyzed to discharge multiple filaggrin repeat subunits (10 to 12 in humans). Filaggrin is highly heterogeneous due to its primary-sequence variability, and numerous degrees of deimination [4]. We assume that the control of filaggrin deimination is a major step in the regulation of its proteolysis, and therefore in the production of NMF amino acids.

Deimination corresponds to the post-translational modification of arginyl to citrullyl residues. It is catalyzed by a family of Ca^{2+}-dependent enzymes called peptidylarginine deiminases (PADs) (E.C. 3.5.3.15). Recently, in our laboratory, the family of human PADs was fully characterized at the genomic level as five clustered paralogous genes (*PADI*1, 2, 3, 4 and 6) on chromosome 1p35-36 [5]. Human PADs are highly conserved, with percentages of identity around 80 % for cDNA and 50 % for amino acid sequences [5–10]. PADs have been detected in numerous organs of humans and rodents by activity measurements and RT-PCR analysis [5, 10–13]. PADs or deimination have been implicated in cutaneous diseases, i.e. psoriasis and bullous congenital ichthyosiform erythroderma [14, 15], in multiple sclerosis [16, 17], in rheumatoid arthritis [18–20] and recently in Alzheimer's disease [21]. Finally, PADs could also be involved in gene regulation since deimination of histones H2A, H3 and H4 has been recently demonstrated and suggested to antagonize arginine methylation-mediated activation of transcription [22–25].

By RT-PCR analysis and immunodetection with specific anti-peptide antibodies, we demonstrated that only PAD1, PAD2 and PAD3 are expressed in normal human and mouse epidermis [5, 10, 26]. The observed co-location of PAD1 and PAD3 with (pro)filaggrin using confocal microscopy argues for their involvement in the deimination of the physiological substrate filaggrin, during epidermal differentiation [26]. However, more direct evidence is lacking and differences between human epidermal PADs in terms of biochemical properties and kinetic parameters have not been published. In this work, using active recombinant isoforms, filaggrin and synthetic substrates, we characterized the properties of the three PADs expressed in the epidermis. Furthermore, the subcellular locations of PAD1 and PAD3 in normal human epidermis were defined by immunoelectron microscopy.

Materials and methods

Antibodies

The monoclonal antibody (mAb) AHF3 is specific to (pro)filaggrin as previously reported [27]. The mAb AHF11 was produced as previously described [27] except that mice were immunized with deiminated filaggrin purified from human epidermis. These mAbs were used at 0.4 μg/ml for western blotting. Specific anti-peptide antibodies directed to PAD1 (anti-PAD1 antibodies) [10] and PAD3 (anti-PAD3 (B3) antibodies) [26] were used for electron microscopy analyses.

Epidermal filaggrin production

Normal adult skin was obtained from plastic surgery after informed consent of patients, conforming to the guidelines of the Declaration of Helsinki. After dermo-epidermal cleavage, an enriched fraction of human filaggrin was produced from the epidermis extracted in a 50 mM Tris-HCl pH 7.4 buffer containing 6 M urea, using a HiTrapQ ion exchange column, as previously described [27]. The fraction was dialyzed against 50 mM Tris-HCl, pH 7.4, and stored at –80 °C.

Affinity chromatography purification of a recombinant filaggrin subunit

A recombinant human filaggrin subunit (GenBank/EMBL/DDBJ accession number AF043380) was produced by fusion with a histidine-tag (His_6) at its N-terminal end (His-filaggrin), in the *Escherichia coli* DH5α strain. The plasmid pOL028 was constructed by subcloning, into the pMR80 vector [28], of a cDNA fragment obtained from pBM163 [29]. Bacteria were cultured at 37 °C in a 2TY medium (Gibco-BRL) with 2 % glucose and 50 μg/ml ampicillin, induced for 3 h with 1 mM isopropyl β-D-thio-galacto-pyranoside (Sigma-Aldrich) and lysed with 0.1 mg/ml lysozyme (Sigma-Aldrich) in phosphate buffer. The bacterial extract was applied to a HiTrap Chelating/Ni^{2+} column (Amersham Biosciences). After washing, the bound proteins were eluted by increasing concentrations of imidazole (50, 200, 350 and 500 mM) (USB Corporation). His-filaggrin-containing fractions were pooled, dialyzed against 50 mM Tris-HCl pH 7.4 and stored at –80 °C.

Production and purification of recombinant human PADs

Recombinant human PAD3 was produced and purified as previously reported [8]. The expression plasmids, pKKhPAD1 and pKKhPAD2, used to produce recombinant human PAD1 and PAD2, were constructed according to a method previously reported [30]. Briefly, the entire coding sequence of *PADI*1 was amplified using the single-stranded cDNA synthesized from cultured normal human epidermal keratinocytes (Clonetics) and a flanking pair of primers designed according to the human *PADI1* cDNA sequence (AB033768) [10]. The 5' primer contained an additional *Eco*RI site, two Shine-Dalgarno sequences and a short cistron. The 3' primer contained an additional *Hin*dIII site. The entire coding region of *PADI2* was amplified, with the same strategy, using a template which was generously provided by Kazusa DNA research institute (Chiba, Japan) (gene name: KIAA0994) and a specific pair of primers. cDNAs were subcloned into

the *Eco*RI/*Hin*dIII sites of the pKK223-3 vector (Amersham Pharmacia Biotech) and their complete sequence confirmed by DNA sequence analysis. Bacterial extracts of *E. coli* JM105 transformed with either pKKhPAD1 or pKKhPAD2 were fractionated by ammonium sulfate precipitation [8]. To purify the recombinant human PAD1, the precipitate was dissolved, dialyzed against buffer A [20 mM Tris-HCl, pH 7.6, 10 mM ethylenediamine tetraacetic acid, 1 mM glycol-bis (β-aminoethyl ether)-tetraacetic acid, 10 mM 2-mercaptoethanol and 0.43 mM phenylmethylsulfonyl fluoride] and applied to an SP-Sepharose Fast Flow column (Amersham Pharmacia Biotech), previously equilibrated with the same buffer. After washing, PAD1 activity was eluted during a linear gradient of 0–0.5 M NaCl. The corresponding fractions were diluted with an equal volume of buffer A containing 3.2 M ammonium sulfate, and applied to a Toyopearl Ether-650M column (Tosoh), previously equilibrated with buffer A containing 1.6 M ammonium sulfate. After washing, PAD1 activity was eluted with a decreasing linear gradient of 1.6–0 M ammonium sulfate. The selected fractions were dialyzed against 6.67 mM MES, 6.67 mM HEPES, 6.67 mM acetate buffer, pH 7.5, and applied to a Poros HS/M Perfusion Chromatography Workstation (BioCAD 700E, PerSeptive Biosystem), previously equilibrated with the same buffer. After washing, PAD1 activity was eluted using a linear gradient of 0–650 mM NaCl. The corresponding fractions were pooled and stored at –80 °C. To purify the recombinant human PAD2, the above procedure was adapted using soybean trypsin inhibitor-agarose affinity column chromatography, as previously described [30].

Substrates of PADs

Filaggrin enriched from human epidermal extracts and His-filaggrin, produced as described above, were used at 5 µg/ml, protamine at 10 mg/ml and synthetic substrates (Bz-L-Arg-O-Et, Bz-L-Arg-O-Me, Bz-L-Arg-O-NH_2, Tos-L-Arg-O-Me, Ac-L-Arg-O-Me, Bz-L-Arg, Ac-L-Arg, L-Arg-O-Me and L-Arg, AC, acetyl; Bz, benzoyl; O-Et, O-ethylester; O-Me, O-methylester; Tos, tosyl) at 10 mM.

Measurement of PAD activities

PAD activities were determined on synthetic L-Arg derivatives as previously described [8, 31]. One unit of enzyme was defined as the amount of PAD able to produce 1 µmol of Bz-L-Cit-O-Et from Bz-L-Arg-O-Et in 1 h at 55 °C [8]. Recombinant and epidermal filaggrin (100 ng/test) were incubated at 50 °C from 0 to 19 h in 100 mM Tris-HCl pH 7.4, 10 mM $CaCl_2$, 5 mM DTT with PAD1, PAD2 or PAD3 (40 milliunits/test). The reactions were stopped by the addition of Laemmli's sample buffer and boiling for 3 min. Proteins were separated by SDS-polyacrylamide gel electrophoresis (SDS-PAGE), electrotransferred to Hybond C-extra reinforced nitrocellulose membranes (Amersham Biosciences) and immunodetected with AHF11. Immunoreactivities were revealed with the ECL-Western blotting detection reagents according to the instructions of the manufacturer (Amersham Biosciences). Deimination of recombinant filaggrin was also measured while varying calcium concentrations (from 0 to 10 mM), adjusting pH (5.2, 7.4, 8.0, or 8.9) in sodium acetate or Tris-HCl buffers, and modifying temperature (22, 37 or 50 °C) in a PCR apparatus.

Quantification of the deimination rate of His-filaggrin

After immunodetection with AHF11, the relative intensity of detected bands was measured using a GeneTools program (Syngene). Images were captured by the Gene Snap system (Syngene), then three areas were defined for each lane: an area at 45 kDa corresponding to the non-deiminated His-filaggrin, an area between 45 and 66 kDa corresponding to partially deiminated forms of His-filaggrin and finally, an area at 66 kDa corresponding to the completely deiminated protein. The relative intensity of each defined area was calculated after background subtraction, expressed as the percentage of the maximal value obtained, and finally reported as the mean ± SD. To obtain accurate determinations, all the experiments corresponding to a given condition were done in parallel for the three PADs, the proteins were simultaneously immunodetected, and the immunoreactivities revealed on the same film. Statistical analyses were performed by unpaired Student's t test. Differences were considered significant when the p value was less than 0.05.

Immunoelectron microscopy analyses

Post-embedding immunoelectron microscopy using Lowicryl HM20 resin (Chemische Werke Lowi) was performed as previously described [32]. Ultrathin sections were prepared, collected on formvar-coated nickel grids, and double labeled with primary antibodies and secondary antibodies conjugated with colloidal gold particles. The specimen-mounted grids were incubated for 15 min at room temperature with pre-incubation buffer (1 % bovine serum albumin, 5 % normal goat serum, 0.1 % fish gelatin, 0.02 % sodium azide in phosphate-buffered saline pH 7.4), then overnight at 4 °C with the anti-PAD1 or anti-PAD3 antibodies diluted to 1:10 or 1:5, respectively, in a first incubation buffer (1 % bovine serum albumin, 1 % normal goat serum, 0.1 % fish gelatin, 0.02 % sodium azide, in phosphate-buffered saline pH 7.4). After washings in the first incubation buffer and the second incubation buffer (1 % bovine serum albumin, 1 % normal goat serum, 0.1 % fish gelatine, in Tris-HCl buffered saline pH 8.2), sections were incubated for 1 h at 37 °C with 5 nm gold-conjugated goat anti-rabbit IgG (Amersham Biosciences) diluted to 1:10 in second incubation buffer. For double labeling, the sections were further incubated

Table 1. Purification of recombinant human PAD1.

Purification step	Total protein (mg)	Total activity* (units)	Specific activity (units/mg protein)	Purity (fold)	Yield (%)
Crude extract	382.0	7240	19	1.0	100
Ammonium sulfate (0–50%)	174.0	6220	36	1.9	86
SP-Sepharose (Fast Flow)	13.6	3790	280	14.8	52
TOYOPEARL Ether-650M	6.6	3290	496	26.2	45
Poros HS/M	5.4	3150	583	30.8	44

* One unit was defined as the amount of PAD1 that catalyzed the formation of 1 μmol of Bz-L-Cit-O-Et from Bz-L-Arg-O-Et in 1 h at 55 °C.

Table 2. Purification of recombinant human PAD2.

Purification step	Total protein (mg)	Total activity* (units)	Specific activity (units/mg protein)	Purity (fold)	Yield (%)
Crude extract	447.0	554	1.2	1.0	100
Ammonium sulfate (0–50%)	221.0	605	2.9	2.3	109
STI-agarose affinity chromatography	0.4	177	434.0	350.0	32

* One unit was defined as the amount of PAD2 that catalyzed the formation of 1 μmol of Bz-L-Cit-O-Et from Bz-L-Arg-O-Et in 1 h at 55 °C.

for 1 h at 37 °C with AHF3 diluted to 1:100, washed as describe above, and incubated for 1 h at 37 °C with 10 nm gold-conjugated goat anti-mouse IgG (Amersham Biosciences) diluted to 1:10. The sections were then contrasted with 1.5% uranyl acetate in methanol. Negative controls corresponded to sections incubated without primary antibodies.

Results

Purification and characterization of active recombinant forms of human epidermal PADs

The recombinant PAD3, the purification of which was previously detailed, showed a specific activity toward Bz-L-Arg-O-Et of 120 units/mg [8]. After ammonium sulfate precipitation (0–50%) of bacterial extracts, recombinant PAD1 and PAD2 were purified by chromatography as summarized in tables 1 and 2, respectively. The final preparations of recombinant PAD1 and PAD2 showed specific activities toward Bz-L-Arg-O-Et of 583 and 434 units/mg, respectively. Figure 1A indicates, by Coomassie blue staining, the purity of the recombinant PAD1, PAD2 and PAD3. Their respective apparent molecular masses were estimated to be 66, 70 and 66 kDa, in agreement with their calculated molecular weights (PAD1: 74, 606; PAD2: 75, 563; PAD3: 74, 770) and the apparent molecular mass of the corresponding isoform detected in human epidermal extracts [26].

Activities and kinetic parameters of the recombinant human PAD1–3

On Bz-L-Arg-O-Et, the maximal activity of purified PAD1 was observed at 50–55°C with a pH optimum at 7.0–7.2. PAD2 showed a maximal activity at 60–65 °C with a range of optimal pH values between 7.0 and 9.0, in accordance with recent published data [33]. As previously reported [8], PAD3 displays an optimum pH of 7.6 with a maximal activity at 50–55 °C. Since PADs were reported to be calcium-dependent enzymes, we tested the effect of various calcium concentrations on each recombinant enzyme at 50 °C, pH 7.4 (fig. 1B). As expected, the three enzymes had an absolute calcium requirement for activity. Very low levels of activity were detected below 1.4 mM calcium for PAD1, 0.4 mM for PAD2, and 3 mM for PAD3. The concentration of calcium necessary to reach the half-maximal relative activity was around 2.5 mM for PAD1, 0.6 mM for PAD2 and 5 mM for PAD3 (fig. 1B). These results were similar to previous data obtained with another recombinant human PAD2 [33] or with native PADs purified from mouse, rat and bovine tissues [13, 34, 35].

We then assessed the activities of the recombinant PAD1, PAD2 and PAD3 toward nine L-Arg derivatives and pro-

Table 3. Kinetic parameters of purified recombinant PAD1, PAD2 and PAD3*.

Substrate	Isoform	Km (mM)	Vmax (µmol/min per milligram	*k*cat (s-1)	*k*cat/Km (s–1 mM–1)
Bz-L-Arg-O-Et	PAD1	0.35	9.09	11.31	32.31
	PAD2	0.50	12.10	15.24	30.48
	PAD3	7.50	1.39	1.73	0.23
Bz-L-Arg	PAD1	0.38	11.60	14.43	37.97
	PAD2	1.49	2.50	3.15	2.11
	PAD3	33.60	0.63	0.79	0.02
Ac-L-Arg-O-Me	PAD1	1.19	9.07	11.28	9.48
	PAD2	3.73	4.94	6.22	1.67
	PAD3	66.30	1.55	1.93	0.03
Ac-L-Arg	PAD1	0.91	11.00	13.68	15.03

* PAD activities were determined at 55 °C for 1 h in 10 mM $CaCl_2$, 10 mM DTT, 100 mM Tris-HCl pH 7.6 buffer containing 10 mM arginine derivatives as described previously [8, 31].

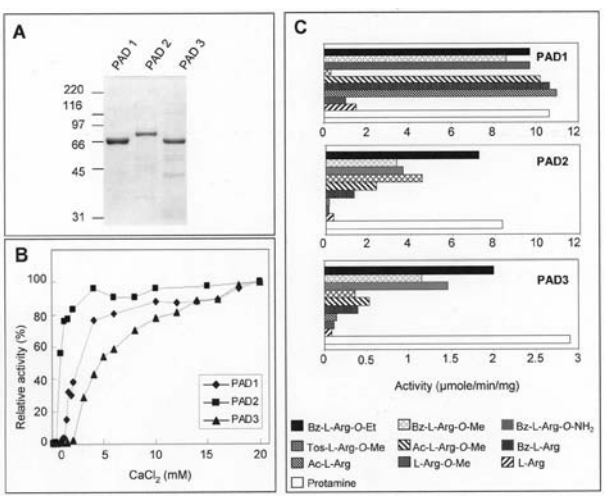

Figure 1. Characterization of recombinant human PAD1, PAD2 and PAD3. (*A*) Coomassie blue staining of purified recombinant human PAD1, PAD2 and PAD3 as indicated at the top of the image. Molecular masses are indicated in kDa on the left. (*B*) Activities of purified recombinant human PAD1 (♦), PAD2 (■) and PAD3 (▲) were measured at 55 °C for 1 h in Tris-HCl pH 7.6 buffer with 10 mM Bz-L-Arg-O-Et as substrate at various concentrations of $CaCl_2$. The relative activities were expressed as the percentage of the maximal activity, for a given isoform. (*C*) Substrate specificities of PAD1, PAD2 and PAD3 were assayed in the same conditions with 10 mM of various L-Arg-derivatives or 10 mg/ml of protamine, as mentioned at the bottom of the histograms, and 10 mM $CaCl_2$. The activities are expressed as the amount of citrulline (in µmol) produced per minute and milligram of recombinant enzyme.

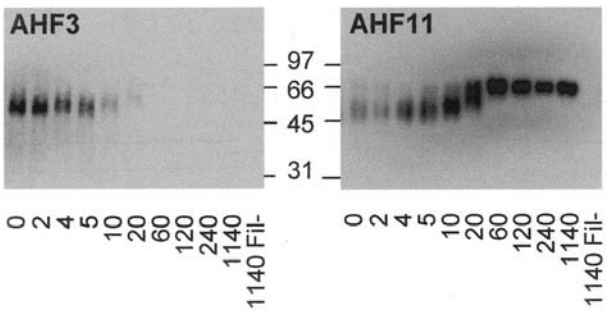

Figure 2. Immunodetection of non-deiminated and deiminated human filaggrin by monoclonal antibodies AHF3 and AHF11. After incubation with PAD1 (40 milliunits/test), human epidermal filaggrin (100 ng/test) was separated by SDS gels and immunodetected with AHF3 and AHF11. Molecular masses are indicated in kDa between the two panels, and incubation times in minutes at the bottom. The last lane of each panel (1140 Fil-) corresponds to a control sample incubated for 1140 min without filaggrin. Note that deimination of filaggrin induces a progressive shift in the apparent molecular mass of the protein from 45 to 66 kDa, inhibits its detection by AHF3 and makes the protein more and more immunoreactive with AHF11.

tamine, a small cationic arginine-rich (63 %) protein (fig. 1C). The three recombinant PADs had low activities if any toward L-arginine and the N-terminal-free small derivative L-Arg-O-Me. Only PAD1 was able to efficiently modify the Ac-L-Arg. Except for Tos-L-Arg-O-Me, PAD1 always showed the highest activity toward the synthetic substrates and protamine. PAD2 was most active on Tos-L-Arg-O-Me, Bz-L-Arg-O-Et and protamine whereas PAD3 showed its highest activities toward Bz-L-Arg-O-NH_2, Bz-L-Arg-O-Et and protamine.

The maximal velocities (V_{max}), K_m and k_{cat} values of recombinant PAD1–3 were assayed with Bz-L-Arg-O-Et, Bz-L-Arg, Ac-L-Arg-O-Me and Ac-L-Arg (table 3). Only PAD1 was observed to catalyze deimination of Ac-L-Arg with measurable K_m and k_{cat} of 0.91 mM and 13.68 s^{-1}, respectively. For the other substrates, PAD3 presented the highest K_m values (7.5–66.3 mM) and PAD1 the lowest (0.35–1.19 mM), showing that PAD1 carries the highest affinities for these substrates. This isoform also showed the best efficiency (kcat/Km values between 9.48 and 37.97 s^{-1} mM^{-1}). Furthermore, PAD3 also presented the lowest V_{max} (0.63–1.55 µmol/min per milligram) and

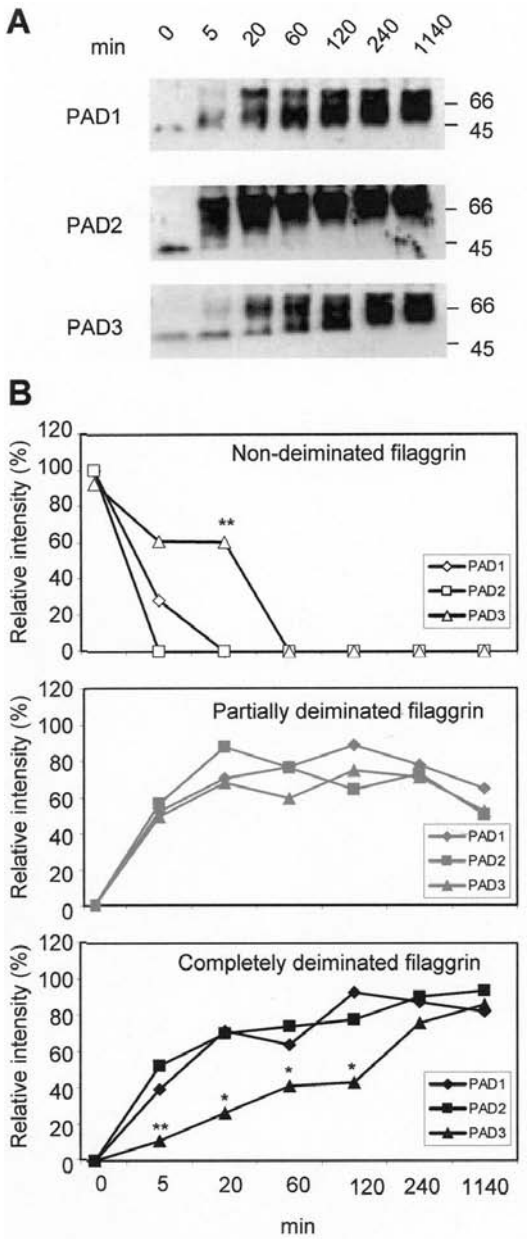

Figure 3. Time courses of filaggrin deimination by PAD1, PAD2 and PAD3. (*A*) His-filaggrin (100 ng/test) was incubated with 40 milliunits/test of either PAD1 (68.6 ng), PAD2 (92.2 ng) or PAD3 (333.3 ng) for 0–1140 min (19 h) at 50 °C in Tris-HCl pH 7.4 buffer containing 10 mM $CaCl_2$, separated by SDS gels and immunodetected with AHF11, a specific mAb for filaggrin, as detailed at the top of representative images. AHF11 reacts more heavily with the complete deiminated His-filaggrin, shifted up to 66 kDa, than with the non-deiminated protein at 45 kDa. Molecular masses are indicated in kDa to the right. (*B*) The relative intensities of the AHF11-immunodetected bands after deimination with PAD1, PAD2 and PAD3 were quantified as described in Materials and methods, and expressed as a percentage of maximal intensity. Open symbols represent non-deiminated His-filaggrin (immunodetected band at 45 kDa), gray symbols are for the partially deiminated His-filaggrin (immunodetected bands between 45 and 66 kDa) and black symbols for the completely deiminated His-filaggrin (immunodetected band at 66 kDa). According to unpaired Student's *t* tests, relative intensities significantly different between isoforms are noted; $^{**}p \leq 0.001$ or $^{*}p \leq 0.05$.

Table 4. Effect of temperature on His-filaggrin deimination by recombinant PAD1–3.

	Relative intensity (%)		
Isoform	22 °C	37 °C	50 °C
PAD1	74.8 ± 19.1	80.4 ± 4.5	87.7 ± 18.5
PAD2	68.6 ± 24.3	98.7 ± 1.9	75.2 ± 18.1
PAD3	73.7 ± 09.7	92.5 ± 7.5	99.6 ± 00.3

His-filaggrin (100 ng/test) was incubated for 19 h at 22, 37 or 50 °C in a PCR apparatus with PAD1, 2 or 3 (40 milliunits/test). After SDS-PAGE and immunodetection with AHF11, relative intensities of the fully deiminated filaggrin were quantified as described in Materials and methods.

k_{cat}/K_m (0.02–0.23 s^{-1} mM^{-1}) values which demonstrated that it is the least efficient isoform to catalyze deimination of small L-Arg-derivatives.

Characterization of a monoclonal antibody highly reactive to deiminated filaggrin

In a series of monoclonal antibodies specific for (pro)filaggrin [27], AHF3 was shown not to detect the deiminated filaggrin. However, AHF11, a new antibody, was able to detect both deiminated and non-deiminated filaggrin, but with a higher reactivity on the former (fig. 2). The deimination of filaggrin induces a progressive shift in its apparent molecular mass from 45 to 66 kDa, as previously observed with native or recombinant proteins, including filaggrin itself [8, 26, 33, 36].

Time courses of filaggrin deimination by recombinant human PAD1–3

To compare the specificity of PAD1, PAD2 and PAD3 for a physiological substrate, a recombinant form of human filaggrin (His-filaggrin) was incubated with the same amount (40 milliunits/test) of the three recombinant isoforms during increasing periods of time and immunodetected with AHF11 (fig. 3). With the three PADs, deimination of His-filaggrin induced the above-described characteristic shift in its apparent molecular mass, from 45 to 66 kDa (fig. 3A). The shift was used to quantify the deimination rate catalyzed by PAD1, PAD2 or PAD3, as described in Materials and methods (fig. 3B). The deimination of His-filaggrin produced by PAD2 was the fastest, whereas the modification by PAD3 was the slowest. Indeed, the maximal amount of deiminated His-filaggrin with PAD3 was observed after 19 h of incubation. By contrast, the maximal amount of deiminated His-filaggrin was observed after 120 min of incubation with PAD1 whereas only 20 min of incubation with PAD2 was necessary to reach the plateau.

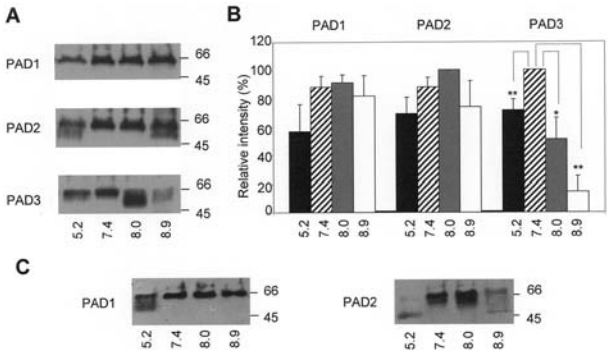

Figure 4. Effect of pH on filaggrin deimination by PAD1, PAD2 and PAD3. (*A*) His-filaggrin (100 ng/test) was incubated either with PAD1, PAD2 or PAD3 (40 milliunits/test) for 19 h at 50 °C in various pH buffers containing 10 mM $CaCl_2$ as detailed at the bottom of representative images obtained after immunodetection with AHF11. Molecular masses are indicated in kDa on the right. (*B*) After incubations with PAD1, PAD2 or PAD3, as indicated at the top of each histogram bar, relative intensities of the completely deiminated filaggrin forms were quantified as described in the legend to figure 3, and are reported as the mean ± SD. According to an unpaired Student's *t* test, for each isoform, relative intensities significantly different between tested pHs, are noted by $^{**}p \leq 0.01$ or $^{*}p \leq 0.05$. (*C*) His-filaggrin was incubated in the same conditions with PAD1 and PAD2 for 1 h or 5 min, respectively. Representative images obtained after immunodetection with AHF11 are shown.

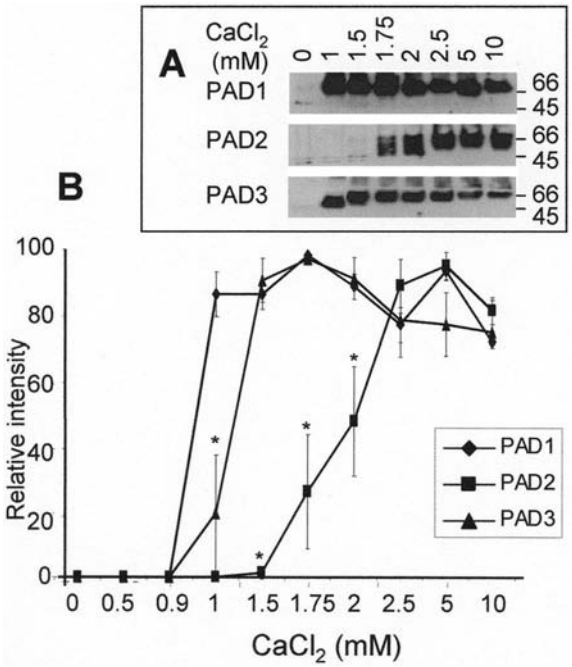

Figure 5. Effect of calcium concentration on filaggrin deimination by PAD1, PAD2 and PAD3. (*A*) His-filaggrin (100 ng/test) was incubated either with PAD1, PAD2 or PAD3, (40 milliunits/test) for 19 h at 50 °C in a Tris-HCl pH 7.6 buffer containing various calcium concentrations between 0 and 10 mM, as detailed at the top of representative images obtained after immunodetection with AHF11. Molecular masses are indicated in kDa on the right. (*B*) After incubations with PAD1(♦), PAD2 (■) and PAD3 (▲), relative intensities of the completely deiminated filaggrin forms were quantified as described in the legend to figure 3, and are reported as the mean ± SD. Relative intensities significantly different between isoforms as determined by Student's unpaired *t* test, are noted by $^{*}p \leq 0.05$.

Furthermore, after 5–120 min of incubation, most His-filaggrin was not or only slightly modified by PAD3, whereas most of the protein was already deiminated by PAD1 and PAD2.

Deimination of filaggrin by PAD1–3 is weakly sensitive to temperature

The deimination of His-filaggrin by recombinant PAD1–3 was assayed after 2 h of incubation at 22, 37 or 50 °C, which corresponds to the mean temperature of the external surface of the skin, the usual physiological temperature and the optimal temperature of PAD activity evaluated with synthetic substrates, respectively. PAD1–3 catalyzed deimination of His-filaggrin at the three temperatures without any statistically significant variations in the activities (table 4).

Deimination of filaggrin by PAD3 is reduced at extreme pH values

The deimination of His-filaggrin was measured after 19 h of incubation with recombinant PAD1, PAD2 or PAD3 at various pH values from 5.2 to 8.9 (fig. 4A, B). PAD1 and PAD2 presented similar activities at the four pH values tested, with a low but not significant decrease in the activities at pH 5.2. By contrast, PAD3 showed an optimum pH at 7.4 and a significant decrease in its activity at the other pH values. The pH sensitivity of the deimination of His-filaggrin by PAD1 and PAD2 was also investigated during shorter incubation periods, either 5 or 60 min (fig. 4C). In these conditions, PAD1 and PAD2 presented lower activities at pH 5.2, but PAD1 was shown to be the least acidity-sensitive isoform. After 1 h of incubation, PAD1 showed the same efficacy at the three higher pH values tested, and a lower activity at the acidic pH. After 5 min of incubation, PAD2 was shown to be efficient at pH 7.4 and 8.0 but displayed low if any activity at the extreme pH values.

Effect of calcium on filaggrin deimination by PAD1–3. The deimination of His-filaggrin by recombinant PAD1, PAD2 or PAD3 was tested at various calcium concentrations between 0 and 10 mM (fig. 5). The deimination of His-filaggrin was not detectable for calcium concentrations between 0 and 0.9 mM. PAD1 needed only 1 mM $CaCl_2$ to produce its maximal activity. PAD3, already efficient at 1 mM $CaCl_2$, exerted its maximal activity at higher concentrations of the ion (1.5 mM). PAD2 needed significantly more $CaCl_2$ to deiminate His-filaggrin since 2.5 mM was necessary to reach its maximal activity. Surprisingly, when tested on Bz-L-Arg-O-Et, the same

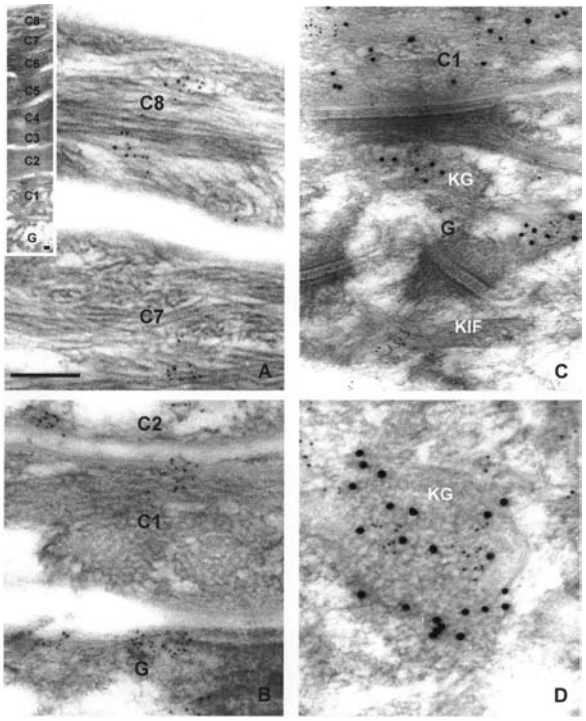

Figure 6. Immunoelectron microscopy localization of PAD1 in human epidermis. C1–C8 indicate the different cornified cell layers; G, granular keratinocyte; KG, keratohyalin granule; KIF, keratin intermediate filaments. Scale bar, 0.1 μ*m (A, B, D)*; 0.2 μm (*C*). (*A, B*), Anti-PAD1 (5-nm gold particles) labeling. (*C, D*), Anti-PAD1 (5-nm gold particles) and AHF3 (10-nm gold particles) double labeling.

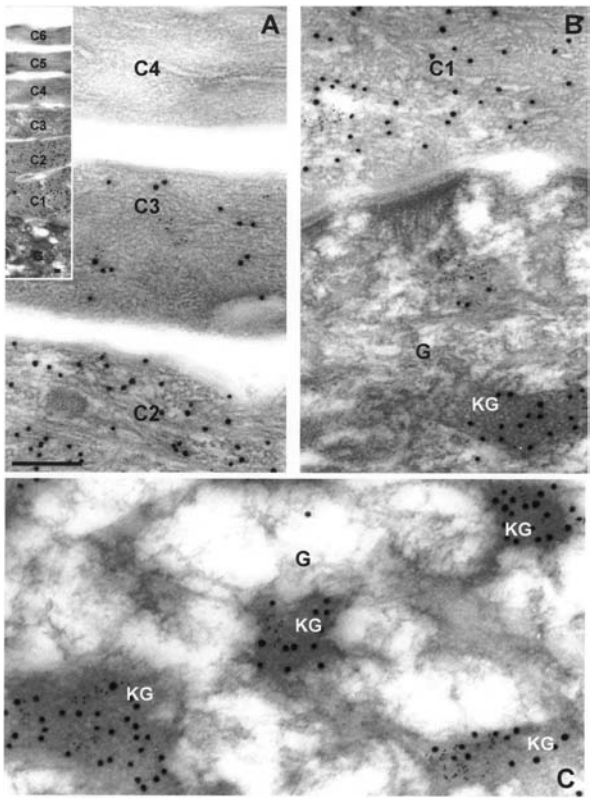

Figure 7. Immunoelectron microscopy localization of PAD3 in human epidermis. C1–C6 indicate the different cornified cell layers; G, granular keratinocyte; KG, keratohyalin granule. Scale bar, 0.2 μm. (*A–C*), Anti-PAD3 (5-nm gold particles) and AHF3 (10-nm gold particles) double labeling.

preparations of recombinant PADs showed maximal activities for concentrations of calcium equal to or higher than 4 mM (fig. 2B). Moreover, PAD3 rather than PAD2 was the isoform that needed the highest calcium concentration to be fully active.

Co-location of PAD1 and PAD3 with filaggrin in the lower SC

The results we obtained *in vitro* did not allow us to discriminate clearly which isoform of PAD deiminates filaggrin *in vivo*, in the lower SC. We therefore investigated whether a particular PAD isoform might be co-located with filaggrin in the epidermis layer. In a previous work, we showed by confocal microscopy that PAD2 is located in the cytoplasm of the lower keratinocytes and at the periphery of the SG keratinocytes; this isoform, therefore, may not be responsible for the deimination of filaggrin [26]. By contrast, PAD1 and PAD3 were shown to be expressed in the cytoplasm of the SG and lower SC cells [26]. To test whether filaggrin and either PAD1 or PAD3 are co-located in normal epidermis, we performed immunoelectron microscopy using a mAb, AHF3, directed to profilaggrin and filaggrin, and anti-peptide antibodies specific to PAD1 or PAD3 (figs. 6, 7).

PAD1 was detected in the cytoplasm of keratinocytes from the basal layer (data not shown) to the SG, and in the intracellular filamentous matrix of corneocytes (fig. 6A, B). PAD1 labeling was retained in the upper layers of the SC, up to the surface of the skin (fig. 6A). In the granular keratinocytes, PAD1 was observed in keratohyalin granules and on keratin intermediate filaments. These results were confirmed, and the co-location of PAD1 with profilaggrin in the granules, and with filaggrin on the corneocyte matrix in the lower SC was demonstrated by double labeling using anti-PAD1 antibodies and AHF3 (fig. 6C, D).

PAD3 labeling was restricted to the SG and lower SC (fig. 7A–C). In the granular keratinocytes, PAD3 was only detected in keratohyalin granules, and the co-location of PAD3 with profilaggrin was clearly demonstrated by double labeling using anti-PAD3 antibodies and AHF3 (fig. 7C). In the SG, PAD3 was never detected on keratin intermediate filaments. PAD3 was observed in the intracellular filamentous matrix of the deeper corneocyte layers (C1–C3, fig. 7A, B), where it was co-located with filaggrin. Both PAD3 and filaggrin labeling disappeared from the fourth layer of corneocytes (C4; fig. 7A).

Discussion

We produced pure and active recombinant human PAD1, PAD2 and PAD3, compared their biochemical activities and physicochemical properties using nine synthetic L-Arg-derivatives, and human filaggrin as a physiological substrate. In addition, immunoelectron microscopy observations were made with specific antibodies to define precisely the subcellular location of PAD1 and PAD3 *in vivo*, and confirmed their potential co-location with filaggrin.

We observed distinct substrate specificities for the three PADs when tested with the synthetic L-Arg-derivatives. The relative activities measured were similar to previously published data obtained with PADs purified from various tissues [11–13, 31]. The few apparent discrepancies observed can be explained either by the origin (human, mouse, rat, bovine or rabbit) or by the degree of purity of the different native enzymes. The three purified human recombinant PADs, produced without any added tag-flag, therefore appeared highly comparable to their corresponding native isoforms. PAD1 needs the L-Arg to be substituted by an α-amino group, with the exception of tosyl, but not by an α-carboxyl group. PAD2 preferentially deiminates the derivatives in which the α-amino and α-carboxyl groups are substituted, and it works better if the α-amino radical is a benzoyl or a tosyl rather than an acetyl. PAD3 needs substitutions at both the α-amino and α-carboxyl ends; concerning the α-carboxyl substituents, this isoform shows a higher activity with the benzoyl group and a lower activity with the tosyl group. We assume from these data that the deimination of an arginyl residue in a given protein is influenced by surrounding amino acids. In agreement, different arginines of Aα and Bβ chains of human fibrinogen were shown to be transformed to citrulline by PAD2 and PAD4 [33]. The same should be true for the deimination of the epidermal substrates, filaggrin and keratins. This would also dictate the specificity of each isoform in terms of physiological substrate choice. These chemical data will also be informative for the design of drugs acting on one PAD without affecting the other isoforms.

The deimination of filaggrin by PAD1, 2 or 3 induces a progressive shift of its migration in SDS gels between 45 to 66 kDa, as previously observed [8, 26, 33, 36]. This is impossible to explain by the theoretical modification of the protein mass alone (1 Da for each citrullyl residue produced, 36 arginyl residues in the protein). A combination of structure and charge changes inducing a progressive unfolding of the progressively deiminated protein may thus be responsible for this unusual mobility alteration, as already proposed [36].

In our *in vitro* assays, PAD2 appears as the most efficient isoform to catalyze the deimination of filaggrin. However, PAD2 has been immunolocalized in the cytoplasm of the lower epidermal keratinocytes and at the periphery of the SG keratinocytes [26]. Therefore it could not act directly on filaggrin *in vivo*. By contrast, the next most efficient PAD, PAD1, was detected in the intracellular filamentous matrix of the deeper corneocytes where it is co-located with filaggrin, as demonstrated by immunoelectron microscopy. These results strongly suggest that PAD1 is involved in the deimination of filaggrin *in vivo*. PAD3 was also detected in the matrix, co-located with filaggrin. Although less active, this isoform is able to deiminate filaggrin *in vitro*. It is therefore very probably involved, like PAD1, in the deimination of filaggrin in the lower SC. The different specificities of these two isoforms, as discussed above, suggest that they deiminate either various arginyl residues on one filaggrin subunit or distinct subunits, the amino acid sequence of which varies from one to the other. Alternatively, this redundancy could be explained by the physiological importance of filaggrin deimination, one enzyme replacing the other if it fails.

PAD1 is the only isoform to be immunodetected in extracts of skin surface samples obtained by tape-stripping [26]. Using immunoelectron microscopy, we confirm that PAD1 is located in the intracellular matrix of corneocytes in the upper SC (fig. 6) where the deiminated keratin K1 has been detected [14, 37, 38]. These results demonstrate that PAD1 is the isoform which deiminates keratin K1 at this skin level. It is probably also involved in the deimination of K10 that seems to occur at this level [38]. In agreement, PAD1 appears to be the least sensitive isoform to acidic pH values and needs the lowest calcium concentration to deiminate a protein. Indeed, the pH of the SC progressively decreases toward the outer surface to reach a mean value of about 5 in the upper most part [39, 40]. However, the acidification does not occur uniformly but through the progressive accumulation of acidic microdomains [39] that may be critical for the regulation of PAD activity. Moreover, the calcium concentration, which is high at the SG and at the deeper SC levels, goes down at the upper SC [41]. Therefore, PAD1 seems to be suited to work in upper-SC conditions.

When we analyzed PADs in detail for their dependence on calcium for activity, we used two substrates, Bz-L-Arg-O-Et (fig. 2) and His-filaggrin (fig. 5). With the synthetic substrate PAD1 showed half-maximal activity at 2.5 mM calcium, PAD2 at 0.6 mM, and PAD3 at 5 mM. When we used filaggrin as a substrate, PAD1 showed half-maximal activity below 1 mM calcium, PAD2 at 2 mM, and PAD3 between 1 and 1.5 mM. This has already been observed with PAD2 purified from mouse muscle and using Bz-L-Arg-O-Et and protamine as substrates [12]. These observations suggest that the calcium sensitivity of PADs depends on the type of substrate, i.e. small synthetic L-Arg-derivatives versus proteins. The reasons for this are unclear; in particular, nothing is known about how

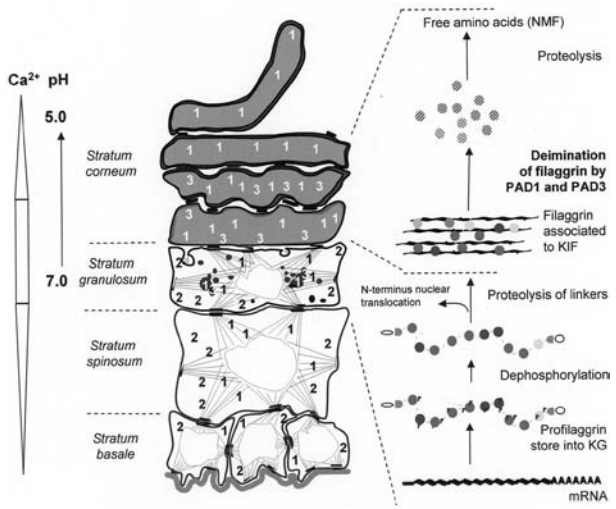

Figure 8. PAD functions in human epidermis and schematic model of filaggrin metabolism up to NMF. PAD1, PAD2 and PAD3 immunolocations are reported by their corresponding numbers (1, 2 and 3, respectively) on an ultrastructural schematic column of keratinocytes from stratum basale to the SC, according to this work and previous data [10, 26]. Nuclei are symbolized by large white areas inside the cells from the stratum basale to the SG. Keratin intermediate filaments (KIFs) are schematized by very fine lines drawn from the nuclear membrane to desmosomes. Keratohyalin granules (KGs) are schematized by black oval structures in the SG. The intracellular fibrous matrix of corneocytes is in gray with the cornified envelope around in black. On the left, Ca^{2+} and pH gradients are symbolized by arrows. On the right, filaggrin metabolism is reported (modified with permission from Pearton et al. [49]). The human filaggrin gene encodes a large precursor profilaggrin of 400 kDa constituted by 10 to 12 filaggrin subunits (gray discs) separated by a unique peptide linker (black bar), surrounded by semi-filaggrin subunits, an N-terminal regulatory domain and a C-terminal tail (white discs). The precursor is expressed in the SG, phosphorylated (p) and stored into KGs. It is then dephosphorylated, before cleavage of filaggrin subunits. During the terminal steps of epidermal differentiation, PAD1 and PAD3 are co-located with profilaggrin in the KGs. In the SG, PAD1 but not PAD3 is also located on KIFs. In the corneocytes of the lower SC, PAD1 and PAD3 are co-located with filaggrin on the intracellular filamentous matrix. There, filaggrin is deiminated, probably by both PAD1 and PAD3. Then, the completely deiminated filaggrin subunits (hatched discs) are proteolyzed to produce the NMF free amino acids. PAD1 is responsible for the deimination of keratin K1, since it is the only isoform present at this level, where deiminated K1 has been previously detected [14, 37, 38].

the structure of the substrates may influence the enzyme activity. In a similar way, the cleavage of small synthetic peptides by kallikrein hKLK5 was shown to be optimal at alkaline pH whereas the cleavage of protein substrates by the same protease proceeds faster at pH 5–7 [42]. The calcium concentrations necessary to measure PAD activities *in vitro* are far from physiological intracellular calcium concentrations, usually evaluated at around 100 nM [43], but local calcium signals could be efficient *in vivo* [44]. Moreover, the increasing calcium gradient from stratum basale to SG, as recently observed by an ion capture cytochemistry method [41], is probably involved in the control of PAD activities. Interestingly, using surface plasmon resonance analysis, an interaction was observed between PAD1 and filaggrin at lower calcium concentration, from 0.1 mM (data not shown). These data suggest that the deimination of filaggrin by PAD1 could start by a phase of interaction or association between the enzyme and its substrate at a low calcium concentration; then the enzyme could need more calcium to display its activity. Recently, the PAD4 crystal structure was resolved and revealed an elongated shape and five Ca^{2+}-binding sites conserved in the other isoforms [45]. Three Ca^{2+}-binding sites were identified in the N-terminal domain, and two in the more conserved C-terminal domain corresponding to the catalytic domain. The former were shown to induce conformational changes of the N-terminal domain and were suspected to be involved in the protein-protein interactions. Our results suggests that the Ca^{2+}-binding sites in the N-terminal domain of PADs may be involved in the association phase with the substrate, whereas the two others may be necessary for the activity itself.

By immunoelectron microscopy, we demonstrated for the first time that PAD1 and PAD3 are located in human epidermal keratohyalin granules (figs. 6, 7). Until now, deiminated proteins have been immunodetected in the rat but not human and mouse epidermal keratohyalin granules. This could be linked to a low sensitivity of the anti-modified citrulline antiserum usually used. Moreover, guinea pig profilaggrin has been shown to be devoid of citrulline, using amino acid composition analysis [4]. A careful check is required whether some keratohyalin granule components are deiminated in human epidermis. One good candidate is a recently identified protein named hornerin whose amino acid composition is close to that of filaggrin and which may share common functions [46]. Interestingly, hornerin seems to be expressed at low levels in normal human skin but up-regulated in psoriatic skin where filaggrin is missing. However, in humans, perinuclear keratohyalin granules of buccal mucosa cells and cytoplasmic granules of cultured epidermis keratinocytes are stained by deiminated filaggrin-specific autoantibodies affinity-purified from rheumatoid arthritis patient sera. The corresponding high-molecular-weight antigens were immunodetected by several anti-(pro)filaggrin monoclonal antibodies and were shown to be biochemically related to deiminated profilaggrin [47, 48]. These data show that profilaggrin can be deiminated on keratohyalin granules during keratinocyte differentiation programs related to but different from epidermis differentiation, in particular when keratinocytes are kept in a highly humid environment. They also strongly suggest that PAD activities might be distinctly regulated depending on the keratinocyte terminal differentiation program, e.g. cornified versus non-cornified epithelia.

Overall, these results allow us to propose a model of PAD1 and PAD3 functions in the human epidermis

(fig. 8). PAD1, immunodetected in the cytoplasm of all epidermis layers from the stratum basale to the SC, may be activated and able to deiminate filaggrin in the lower SC. Indeed, it is co-located with filaggrin on keratin intermediate filaments at this level. PAD3 is probably involved in filaggrin deimination as well since it is also co-located with the protein in the lower SC. Then, deiminated filaggrin is proteolyzed to produce the free aminoacids of the NMF necessary to maintain the hydration of the SC and homeostasis of the epidermis. Since PAD1 is active at the acidic pH of the upper SC and is the sole isoform immunodetected at this level, where deiminated keratin K1 is observed, PAD1 is the isoform responsible for the deimination of this keratin. It is probably also involved in the deimination of K10 in the upper SC. Keratin K1 deimination has been shown to be concomitant with a rearrangement of the intracellular matrix of the corneocytes, from reticular to amorphous [14]. This suggests that the keratin modification achieved by PAD1 is involved in such an observed ultrastructural change.

In summary, human PAD1, 2 and 3 show different enzymatic properties including substrate specificities, tissue and cellular distributions, and physicochemical condition dependencies. This suggests different functions for the various PAD isoforms despite their 50–55 % amino acid sequence identity. Since the high-resolution structure of PAD4 is now resolved, it may help us to understand these differences by *in silico* modeling.

Although, in the epidermis, deimination is involved in the regulation of SC hydration, reorganization of corneocyte filamentous matrix and therefore maintenance of the barrier function, the role of this post-translational modification in the other tissues is still unclear. To better understand the physiological role(s) of PADs and their involvement in diseases, and to be able in the future to regulate abnormal deimination, we need to decipher the way their expression is regulated and their activity modulated.

Acknowledgments. We thank C. Pons for her excellent technical assistance, J. Arnaud for his helpful assistance with Syngene's programms, L. Laval and D. Morel for their technical help and C. Vincent for the drawing of the original ultrastructural schematic column of keratinocytes. pOL028 was a kind gift of M. Jolivet's team at Biomérieux Research Laboratories (Marcy-L'Etoile, France). The electron microscopy samples were observed at the Electron Microscopy Unit of the Central Laboratory for Research and Education at Asahikawa Medical College (Asahikawa, Japan). R. N. is grateful to M. Haftek from Lyon (France) for initiating her to immunoelectron microscopy. This work was supported by grants from the Centre National de la Recherche Scientifique (CNRS), the European Regional Development Funds (ERDF), the European Social Funds (ESF), the Institut National de la Santé et de la Recherche Médicale (INSERM), the Société de Recherche Dermatologique (SRD) and from the Centre Européen de Recherche sur la Peau et les Epitheliums de Revêtement (CERPER, Toulouse, France).

1 Madison K. C. (2003) Barrier function of the skin: "la raison d'être" of the epidermis. J. Invest. Dermatol. **121:** 231–241
2 Rawlings A. V. and Harding C. R. (2004) Moisturization and skin barrier function. Dermatol. Ther. **17:** 43–48
3 Scott I. R., Harding C. R. and Barrett J. G. (1982) Histidine-rich protein of the keratohyalin granules. Source of the free amino acids, urocanic acid and pyrrolidone carboxylic acid in the stratum corneum. Biochim. Biophys. Acta **719:** 110–117
4 Harding C. R. and Scott I. R. (1983) Histidine-rich proteins (filaggrins): structural and functional heterogeneity during epidermal differentiation. J. Mol. Biol. **170:** 651–673
5 Chavanas S., Méchin M. C., Takahara H., Kawada A., Nachat R., Serre G. et al. (2004) Comparative analysis of the mouse and human peptidylarginine deiminase gene clusters reveals highly conserved non-coding segments and a new human gene, PADI6. Gene **330:** 19–27
6 Nakashima K., Hagiwara T., Ishigami A., Nagata S., Asaga H., Kuramoto M. et al. (1999) Molecular characterization of peptidylarginine deiminase in HL-60 cells induced by retinoic acid and 1alpha,25-dihydroxyvitamin D(3). J. Biol. Chem. **274:** 27786–27792
7 Rus'd A. A., Ikejiri Y., Ono H., Yonekawa T., Shiraiwa M., Kawada A. et al. (1999) Molecular cloning of cDNAs of mouse peptidylarginine deiminase type I, type III and type IV, and the expression pattern of type I in mouse. Eur. J. Biochem. **259:** 660–669
8 Kanno T., Kawada A., Yamanouchi J., Yosida-Noro C., Yoshiki A., Shiraiwa M. et al. (2000) Human peptidylarginine deiminase type III: molecular cloning and nucleotide sequence of the cDNA, properties of the recombinant enzyme, and immunohistochemical localization in human skin. J. Invest. Dermatol. **115:** 813–823
9 Ishigami A., Ohsawa T., Asaga H., Akiyama K., Kuramoto M. and Maruyama N. (2002) Human peptidylarginine deiminase type II: molecular cloning, gene organization, and expression in human skin. Arch. Biochem. Biophys. **407:** 25–31
10 Guerrin M., Ishigami A., Méchin M. C., Nachat R., Valmary S., Sebbag M. et al. (2003) cDNA cloning, gene organization and expression analysis of human peptidylarginine deiminase type I. Biochem. J. **370:** 167–174
11 Watanabe K., Akiyama K., Hikichi K., Ohtsuka R., Okuyama A. and Senshu T. (1988) Combined biochemical and immunochemical comparison of peptidylarginine deiminases present in various tissues. Biochim. Biophys. Acta. **966:** 375–383
12 Takahara H., Tsuchida M., Kusubata M., Akutsu K., Tagami S. and Sugawara K. (1989) Peptidylarginine deiminase of the mouse: distribution, properties, and immunocytochemical localization. J. Biol. Chem. **264:** 13361–13368
13 Terakawa H., Takahara H. and Sugawara K. (1991) Three types of mouse peptidylarginine deiminase: characterization and tissue distribution. J. Biochem. (Tokyo) **110:** 661–666
14 Ishida-Yamamoto A., Senshu T., Eady R. A., Takahashi H., Shimizu H., Akiyama M. et al. (2002) Sequential reorganization of cornified cell keratin filaments involving filaggrin-mediated compaction and keratin 1 deimination. J. Invest. Dermatol. **118:** 282–287
15 Ishida-Yamamoto A., Senshu T., Takahashi H., Akiyama K., Nomura K. and Iizuka H. (2000) Decreased deiminated keratin K1 in psoriatic hyperproliferative epidermis. J. Invest. Dermatol. **114:** 701–705
16 Moscarello M. A, Wood D. D., Ackerley C. and Boulias C. (1994) Myelin in multiple sclerosis is developmentally immature. J. Clin. Invest. **94:** 146–154.
17 Kim J. K., Mastronardi F. G., Wood D. D., Lubman D. M., Zand R. and Moscarello M. A. (2003) Multiple sclerosis: an important role for post-translational modifications of myelin basic protein in pathogenesis. Mol. Cell. Proteomics **2:** 453–462
18 Masson-Bessière C., Sebbag M., Girbal-Neuhauser E., Nogueira L., Vincent C., Senshu T. et al. (2001) The major synovial targets of the rheumatoid arthritis-specific antifilaggrin autoan-

tibodies are deiminated forms of the alpha- and beta-chains of fibrin. J. Immunol. **166:** 4177–4184
19 Vossenaar E. R., Zendman A. J., Venrooij W. J. van and Pruijn G. J. (2003) PAD, a growing family of citrullinating enzymes: genes, features and involvement in disease. Bioessays **25:** 1106–1118
20 Sebbag M., Chapuy-Regaud S., Auger I., Petit-Texeira E., Clavel C., Nogueira L. et al. (2004) Clinical and pathophysiological significance of the autoimmune response to citrullinated proteins in rheumatoid arthritis. Joint Bone Spine **71:** 493–502
21 Ishigami A., Ohsawa T., Hiratsuka M., Taguchi H., Kobayashi S., Saito Y. et al. (2005) Abnormal accumulation of citrullinated proteins catalyzed by peptidylarginine deiminase in hippocampal extracts from patients with Alzheimer's disease. J. Neurosci. Res. **80:** 120–128
22 Nakashima K., Hagiwara T. and Yamada M. (2002) Nuclear localization of peptidylarginine deiminase V and histone deimination in granulocytes. J. Biol. Chem. **277:** 49562–49568
23 Cuthbert G. L., Daujat S., Snowden A. W., Erdjument-Bromage H., Hagiwara T., Yamada M. et al. (2004) Histone deimination antagonizes arginine methylation. Cell **118:** 545–553
24 Sarmento O. F., Digilio L. C., Wang Y., Perlin J., Herr J. C., Allis C. D. et al. (2004) Dynamic alterations of specific histone modifications during early murine development. J. Cell Sci. **117:** 4449–4459
25 Wang Y., Wysocka J., Sayegh J., Lee Y. H., Perlin J. R., Leonelli L. et al. (2004) Human PAD4 regulates histone arginine methylation levels via demethylimination. Science **306:** 279–283
26 Nachat R., Méchin M. C., Takahara H., Chavanas S., Charveron M., Serre G. et al. (2005) Peptidylarginine deiminase isoforms 1-3 are expressed in the epidermis and involved in the deimination of k1 and filaggrin. J. Invest. Dermatol. **124:** 384–393
27 Simon M., Sebbag M., Haftek M., Vincent C., Girbal-Neuhauser E., Rakotoarivony J. et al. (1995) Monoclonal antibodies to human epidermal filaggrin, some not recognizing profilaggrin. J. Invest. Dermatol. **105:** 432–437
28 Cheynet V., Verrier B. and Mallet F. (1993) Overexpression of HIV-1 proteins in *Escherichia coli* by a modified expression vector and their one-step purification. Protein. Expr. Purif. **4:** 367–372
29 Girbal-Neuhauser E., Durieux J. J., Arnaud M., Dalbon P., Sebbag M., Vincent C. et al. (1999) The epitopes targeted by the rheumatoid arthritis-associated antifilaggrin autoantibodies are posttranslationally generated on various sites of (pro)filaggrin by deimination of arginine residues. J. Immunol. **162:** 585–594
30 Ohsugi I., Takahara H., Shiraiwa M. and Sugawara K. (1995) Expression of mouse uterine peptidylarginine deiminase in *Escherichia coli:* construction of expression plasmid and properties of the recombinant enzyme. Arch. Biochem. Biophys. **317:** 62–68
31 Takahara H., Oikawa Y. and Sugawara K. (1983) Purification and characterization of peptidylarginine deiminase from rabbit skeletal muscle. J. Biochem. (Tokyo) **94:** 1945–1953
32 Nakane H., Ishida-Yamamoto A., Takahashi H., and Iizuka H. (2002) Elafin, a secretory protein, is cross-linked into the cornified cell envelopes from the inside of psoriatic keratinocytes. J. Invest. Dermatol.**119:** 50–55
33 Nakayama-Hamada M., Suzuki A., Kubota K., Takazawa T., Ohsaka M., Kawaida R. et al. (2005) Comparison of enzymatic properties between hPADI2 and hPADI4. Biochem. Biophys. Res. Commun. **327:** 192–200
34 Fujisaki M. and Sugawara K. (1981) Properties of peptidylarginine deiminase from the epidermis of newborn rats. J. Biochem. (Tokyo) **89:** 257–263
35 Lamensa J. W. and Moscarello M. A. (1993) Deimination of human myelin basic protein by a peptidylarginine deiminase from bovine brain. J. Neurochem. **61:** 987–996
36 Tarcsa E., Marko L. N., Mei G., Melino G., Lee S. C. and Steinert P. M. (1996) Protein unfolding by peptidylarginine deiminase: substrate specificity and structural relationships of the natural substrates trichohyalin and filaggrin. J. Biol. Chem. **271:** 30709–30716
37 Senshu T., Akiyama K., Ishigami A. and Nomura K. (1999) Studies on specificity of peptidylarginine deiminase reactions using an immunochemical probe that recognizes an enzymatically deiminated partial sequence of mouse keratin K1. J. Dermatol. Sci. **21:** 113–126
38 Senshu T., Kan S., Ogawa H., Manabe M. and Asaga H. (1996) Preferential deimination of keratin K1 and filaggrin during the terminal differentiation of human epidermis. Biochem. Biophys. Res. Commun. **225:** 712–719
39 Behne M. J., Meyer J. W., Hanson K. M., Barry N. P., Muruta S., Crumrine D. et al. (2002) NHE1 regulates the stratum corneum permeability barrier homeostasis. J. Biol. Chem. **277:** 47399–47406
40 Matousek J. L. and Campbell K.L. (2002) A comparative review of cutaneous pH. Vet. Dermatol. **13:** 293–300
41 Bikle D.D., Oda Y. and Xie Z. (2004) Calcium and 1,25(OH)(2)D: interacting drivers of epidermal differentiation. J. Steroid Biochem. Mol. Biol. **89:** 355–360
42 Brattsand M., Stefansson K., Lundh C., Haasum Y. and Egelrud T. (2005) A proteolytic cascade of kallikreins in the stratum corneum. J. Invest. Dermatol. **124:** 198–203
43 Clapham D. E. (1995) Calcium signaling. Cell 80: 259–268
44 Bootman M. D., Lipp P. and Berridge M. J. (2001) The organisation and functions of local Ca(2+) signals. J. Cell Sci. **114:** 2213–2222
45 Arita K., Hashimoto H., Shimizu T., Nakashima K., Yamada M. and Sato M. (2004) Structural basis for Ca(2+)-induced activation of human PAD4. Nat. Struct. Mol. Biol. **11:** 777–783.
46 Takaishi M., Makino T., Morohashi M. and Huh N. H. (2005) Identification of human hornerin and its expression in regenerating and psoriatic skin. J. Biol. Chem. **280:** 4696–4703
47 Sebbag M., Simon M., Vincent C., Masson-Bessiere C., Girbal E., Durieux J. J. et al. (1995) The antiperinuclear factor and the so-called antikeratin antibodies are the same rheumatoid arthritis-specific autoantibodies. J. Clin. Invest. **95:** 2672–2679
48 Girbal-Neuhauser E., Montézin M., Croute F., Sebbag M., Simon M., Durieux J. J. et al. (1997) Normal human epidermal keratinocytes express *in vitro* specific molecular forms of (pro)filaggrin recognized by rheumatoid arthritis-associated antifilaggrin autoantibodies. Mol. Med. **3:** 145–156
49 Pearton D. J., Dale B. A. and Presland R. B. (2002) Functional analysis of the profilaggrin N-terminal peptide: identification of domains that regulate nuclear and cytoplasmic distribution. J. Invest. Dermatol. **119:** 661–669